Unstable Vortices in the Near Region of an Internal Flow Cavity

L. K. Isaacson,* M. K. Denison,† and J. C. Crepeau‡
University of Utah, Salt Lake City, Utah

This paper presents experimental data taken in the forward region of a separated internal free-shear layer produced in an internal cavity flowfield. It has been found that in the region very near the forward restrictor, experimental velocity profiles agree closely with the exact Stuart instability velocity profile with various values of a steepness parameter. Reynolds shear-stress profiles suggest the presence of counter-rotating longitudinal vortices. Spectral analysis by the maximum entropy method of the time samples within the vortices indicates subharmonic and harmonic components of the fundamental frequency, with a weak indication of the fundamental frequency itself.

I. Introduction

INTERNAL flow cavity configurations occur in many engineering applications, from segmented solid propellant rocket motors to dump combustors in ramjet engines. A recent review[1] indicates that information concerning the characteristics of the shear layers at the leading edge of flow cavities is not sufficiently detailed to identify clearly the physical mechanisms involved in shear layer instability and transition. The objective of this paper is to present experimental measurements of the flow field in the near region of an internal cavity flow. The results presented suggest the occurrence of unstable spiral vortices in the steep shear layers very near the forward restrictors in an internal flow cavity.

The near region of the free-shear layer in an internal cavity flow plays an important role in the development of the downstream characteristics of the flow, especially in regard to the formation of axially directed spiral vortices and large, spanwise roll vortices. There is an important need to understand the processes that occur very near the forward restrictors in an internal cavity flow, a region in which the velocity profiles are very steep, and in which three-dimensional instabilities are in evidence. For the flow configuration used here, as indicated in Figs. 1 and 2, the presence of a beveled edge on the upstream side of each of the upper and lower forward restrictors produces a flow along separation lines away from the forward bevel lines, and over the sharp edges of the restrictors. The flow over each of the restrictors appears to be similar to the flow of parallel streams as studied by Stuart.[2] Comparison of measured velocity profiles with the profiles of Stuart show excellent agreement.

Profiles of Reynolds shear stress in the forward region of the cavity flow show evidence of axially directed, counter-rotating vortices produced along the shear layer that are time-dependent and that rapidly move apart in the downstream direction. We have characterized these flow structures as unstable velocity bursts. Time samples of the axial velocity signals within the bursts were obtained, and the maximum entropy method was applied to these samples to obtain the dominant frequencies within the bursts. These results indicate the presence of both subharmonic and superharmonic components of the most unstable frequency as demonstrated by Miksad[3] for the tanh (y) profiles. Frequency components in the range of two-dimensional Tollmein-Schlichting waves were limited in extent.

II. Experimental Procedures

Experiments were conducted in a subsonic wind tunnel at the University of Utah. A schematic diagram of the wind-tunnel facility is shown in Fig. 1. The test section is 2.44 m in length, and has a cross section of 180 mm on each side. A schematic diagram of the flow cavity is presented in Fig. 2. Note that the forward pair of restrictors is located 1.91 m downstream from the entrance to the test section. We should also note that the first 0.61 m of the top surface of the test section is covered with sandpaper to enhance the transition to turbulence along the upper sufrace. The purpose of enhancing the transition process is to assure a turbulent boundary layer along the upper wall while the flow along the lower wall remains essentially laminar. A significant aspect for studies within this facility has been the characteristics of asymmetric flows of the type produced by the presence of the sandpaper. In this paper, however, we are concerned primarily with the characteristics of the laminar flow over the forward restrictor on the lower side of the tunnel.

The axial and vertical velocities within the steep shear layer were measured with an X-configuration, constant temperature, hot-film anemometer. The anemometer was placed at various stations downstream from the forward (right-hand side) restrictor. The value of the mean velocity at each vertical point was taken as an average of 50 samples. One-thousand vertical steps were made in increments of 0.08 mm using a computer-controlled stepper motor-driven traversing mechanism, amounting to a total of 80 mm from the upper region to the lower region of the flow cavity. The vertical extent covered by the profiles is shown in Fig. 2.

The X-configuration probe used in these measurements was a TSI Model 1251A-20 hot-film boundary-layer probe. In order to analyze the anemometer signals, two TSI Model 1050 Constant Temperature Anemometers, two TSI Model 1055 Linearizers, and a TSI Model 1015C Sum and Difference Circuit were used. Digital processing and analog data reduction were done with a Hewlett-Packard Model 2240A Measurement and Control Processor, a Hewlett-Packard HP-85B Controller, and a Hewlett-Packard 7225A x-y plotter.

A Princeton Applied Research Model 162 Boxcar Averager with two Model 164 Gated Integrator Modules and a product

Received Aug. 1, 1988; revision received Feb. 11, 1989.

*Professor, Department of Mechanical Engineering. Associate Fellow AIAA.

†Currently, Member of the Technical Staff, Jet Propulsion Laboratory, Pasadena, CA.

‡Graduate Student, Department of Mechanical Engineering. Student Member AIAA.

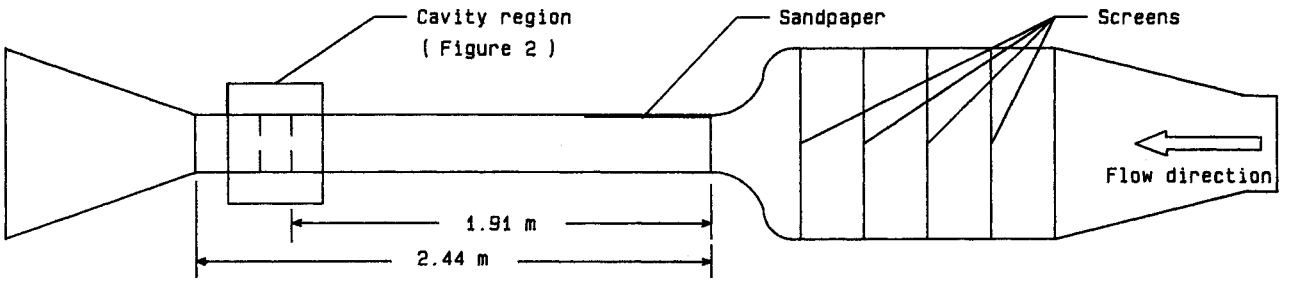

Fig. 1 Schematic diagram of the subsonic wind-tunnel facility. The schematic is not to scale.

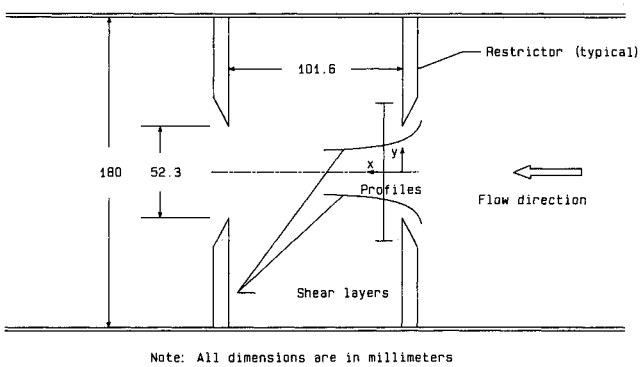

Fig. 2 Schematic diagram of the internal flow cavity.

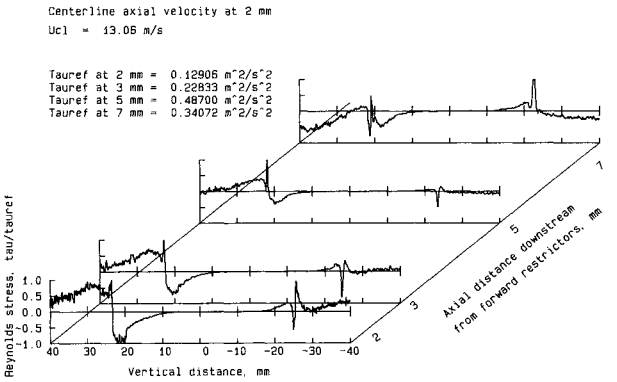

Fig. 3 Reynolds shear-stress profiles across the central 80 mm of the flow channel at axial stations of 2, 3, 5, and 7 mm downstream from the forward restrictors.

option were used as a cross correlator to obtain measurements of the Reynolds stress across the central flow channel. A TSI Model 1064 Correlator was used to obtain products of fluctuating velocities, and a TSI Model 1015 Time-Differentiation circuit together with the PAR Model 162 Boxcar Averager were used to obtain both mean values and conditioned values of the turbulence energy dissipation rates at selected locations within the shear layers. Taylor's hypothesis was used to relate the time-differentiated velocities to the turbulence energy dissipation rates.

A Hewlett-Packard Model 3582A Spectrum Analyzer was used to obtain the time samples used in the evaluation of turbulent bursts in the forward region of the lower shear layer. The Model 3582A provided 1024 samples in 10 ms, a sampling rate giving excellent resolution of the turbulent bursts observed in this region.

III. Results and Discussion

Figure 3 indicates profiles of the Reynolds shear stress across the central 80 mm of the channel at four axial stations, at distances of 2, 3, 5, and 7 mm downstream of the forward restrictors. The shear-stress profiles reflect the turbulent nature of the upper boundary layer as compared with the more laminar lower boundary layer. The lower surface of the wind tunnel is smooth so that the lower boundary layer remains essentially laminar going into the internal flow cavity. In the present comparison, the shear layer over the lower restrictor edge is considered as an internal free shear layer, which is approximated as a mixing layer between two viscous streams. This shear layer is inherently unstable, with instabilities developing along the layer in the downstream direction. As these instabilities grow, they begin to distort the velocity profile, and a comparison of the experimental velocity profiles with the theoretical analysis of Stuart[2] becomes of interest.

The stream function Ψ for a free shear layer derived by Stuart is

$$\Psi = cy + \ell n\,[C\cosh(y) + A\cos(x - ct)] \qquad (1)$$

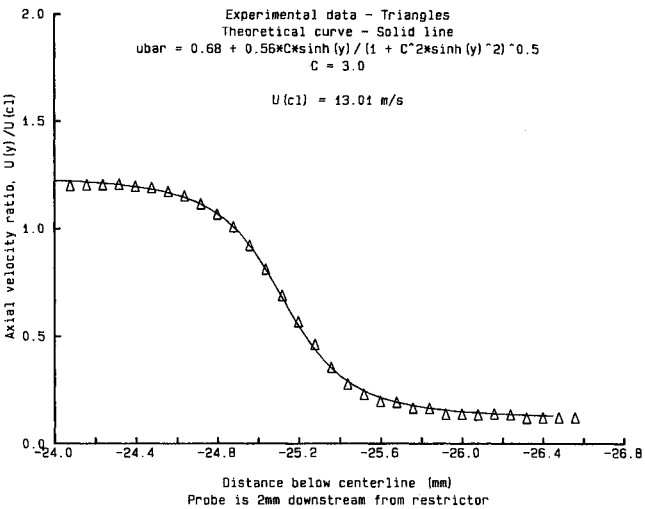

Fig. 4 Comparison of experimental and theoretical velocity profiles through the lower shear layer at an axial station of 2 mm downstream of the forward restrictors. The theoretical solution is based upon Stuart's analysis of mixing layers, with $C = 3.0$.

where x is in the axial direction and y is in the vertical direction. After taking the derivative of Ψ with respect to y and averaging over several repeated cycles in the downstream or axial direction, Stuart found an exact closed form expression for the local mean velocity as,

$$\bar{u} = c + k\,\frac{C\sinh(y)}{(1 + C^2\sinh^2 y)^{1/2}} \qquad (2)$$

where c is a positioning constant, k is a scaling parameter, and C determines the slope of the shear layer velocity profile. Figure 4 presents normalized mean velocity values from the experimental velocity profile at 2 mm downstream of the for-

Table 1 Displacement thickness, momentum thickness, and Reynolds number

Axial station, mm	Displacement thickness, δ^*, mm		Momentum thickness, θ, mm		δ^*/θ		Reynolds number, Re_θ	
	Upper layer	Lower layer	Upper layer	Lower layer	Upper layer	Lower layer	Upper layer	Lower layer
2	0.905	1.05	0.274	0.250	3.31	4.20	221	218
3	0.909	1.27	0.275	0.277	3.30	4.59	231	250
5	1.170	1.46	0.360	0.320	3.26	4.58	312	229
7	2.000	2.79	0.561	0.583	3.56	4.78	499	534
12	4.060	4.91	1.020	1.000	3.96	4.91	984	955
18	5.550	5.73	1.410	1.260	3.93	4.54	1341	1216
28	5.680	8.25	1.600	1.790	3.54	4.60	1598	1794

Table 2 Theoretical frequencies based on $St_\theta = 0.0177$

Axial station, mm	fn, Hz	$fn/2$ Hz	$fn/4$ Hz	$3fn/2$ Hz	$5fn/2$ Hz	$7fn/2$ Hz
			Upper layer			
2	937	469.0	234	1406	2343	3280
3	970	485.0	243	1455	2425	3395
5	772	386.0	193	1158	1930	2702
7	509	255.0	127	764	1273	1782
12	296	148.0	73.9	444	740	1036
18	215	108.0	53.8	323	538	753
28	197	98.7	49.4	296	493	690
			Lower layer			
2	1110	555.0	277.0	1664	2775	3885
3	1035	518.0	259.0	1553	2588	3623
5	938	469.0	235.0	1407	2345	3283
7	505	252.0	126.0	757	1263	1768
12	302	151.0	75.4	452	755	1057
18	244	122.0	60.9	366	610	854
28	178	88.8	44.4	267	445	623

ward restrictor and results obtained from Eq. (2). These results indicate excellent agreement between the Stuart profile, shown as a solid line, and the experimental data, shown in triangles. For the experimental results shown in Fig. 4, the normalizing centerline velocity was 13.01 m/s. Note that the value for the scaling parameter, k, of 0.56 in Fig. 4 scales the range of the hyperbolic function in Eq. (2), (which is -1.0 to 1.0) to the range of the experimental velocity ratios of 0.2 to 1.2.

When correlating the Stuart theoretical profile with experimental data, the parameter C in Eq. (2) determines the slope of the theoretical velocity profile. For large values of C, the profiles of Eq. (2) become very steep. As C approaches unity, the profiles approach the hyperbolic tangent profile. For the velocity profiles measured in this facility, the value of C was typically found to be between 3 and 2. In Fig. 4, the value of C was determined to be 3.0. As the flow moves downstream, viscous interaction between the two streams changes the velocity profile. It was found that the parameter C decreases for stations axially downstream. For the velocity profile at a downstream station of 3 mm, with a centerline velocity of 13.3 m/s, the Stuart parameter C was determined to be 3.0. At the downstream station of 5 mm and the centerline velocity of 13.77 m/s, C decreases to 2.8. At 7 mm, C has decreased further to 2.2, with the velocity along the center line increasing to 14.24 m/s.

Thus, following the interpretation of Stuart,[2] the flow initially represents a sheet of point vortices along the critical layer, representing a line of separation of the flow. Viscous interaction modifies the shear layer, introducing instabilities along the layer, until C approaches unity, which then represents the viscous shear layer hyperbolic tangent profile.

We should note that the Stuart analysis does not include a number of effects that are present in the experimental flow used in this experiment. First, the steep shear layers coming into the flow cavity are curved, which introduces nonparallel effects into the flow. However, Wooley and Karamcheti[4] have shown that the stability characteristics of nonparallel shear layers are closely related to those of parallel shear layers. Hence, agreement of the Stuart results with the experimental profiles as shown here provides support for the application of the Stuart profiles in the development of deterministic analyses. Second, the internal static pressure is decreasing along the flow centerline toward the center of the cavity. Finally, the flow velocity decreases from the center of the cavity toward the rear restrictors, resulting in an increasing static pressure toward the rear restrictors. As large-scale vortices interact with the downstream restrictors, acoustical pressures may be produced within the flow cavity. We have operated the flow facility at velocities just below the threshold at which measurable acoustic energy is produced within the flow cavity. In view of these additional conditions, we have attempted to present the experimental data without modification, reflecting the experimental conditions as measured at the various stations in the near region of the forward restrictors.

In a study directed toward the extension of deterministic methods to actual engineering applications (Crepeau and Isaacson[5]), the close agreement of the theoretical Stuart profile with the measured velocity profiles led to the use of the Stuart equation as a means to calculate velocity gradients within the shear layer at various axial and vertical stations. The velocity profiles represented by the Stuart relationship were used to represent the velocity gradients in the Townsend[6] expansion of the Navier-Stokes equations. The integration with time of the resulting set of coupled first-order differential equations indicates that the velocity profiles established along the near-region shear layers produce "regions of instability," which, in a deterministic approach, show unstable behavior leading to the production of rapidly changing velocity components. Outside of these regions, the flow is stable, and the velocity components behave smoothly.

IV. Theoretical Fundamental Frequencies

In Table 1, we have presented the displacement thicknesses for both the upper and lower shear layers, the momentum thicknesses, the ratios of displacement and momentum thicknesses, and the Reynolds number based on the peak velocity in the shear layer and the momentum thickness of the shear layer. Table 2 gives theoretical frequencies for the most unstable of the disturbances of the tanh (y) type velocity profiles (Miksad),[3] which correspond with the results obtained in our experimental configuration. The resonant frequencies are calculated from the expression

$$fn = St\ U_T/\theta_m \tag{3}$$

where St is the Strouhal number, $St_\theta = 0.0177$ for the most unstable disturbance in the shear layer from Michalke's results,[7] U_T is the measured maximum velocity on the freestream

side of the shear layer, and θ_m is the momentum thickness evaluated from the measured velocity profile through the lower shear layer. The subharmonics, $fn/2$, $fn/4$, $3fn/2$, $5fn/2$, and $7fn/2$, are presented for comparison with the results obtained from the maximum entropy analysis of the unstable bursts observed in the lower shear layer.

Note that as the measured momentum thickness increases in the axial direction, the predicted instability frequency decreases. At a distance of 28 mm from the forward restrictors, the predicted instability frequency has decreased to 178 Hz, which is of the order of frequency of the subsonic facility. The centerline velocity at the forward restrictors was held at 13.01 m/s for the measurements reported here, lower than the velocity at which acoustical oscillations are produced within the cavity. Extending the trend then indicates that for slightly higher tunnel velocities, instability frequencies of the order of 168 Hz may be reached within the distance of 28 mm. Intense acoustical oscillations at a frequency of 168 Hz are produced in this facility at tunnel centerline velocities higher than 17 m/s at 2 mm downstream of the forward restrictors.

V. Unstable Bursts in an Internal Free-Shear Layer

Early analyses of the turbulent burst phenomenon by Benney[8,9,10] and Greenspan and Benney[11] indicate that steep shear layers of the type observed here could give rise to unstable bursts which could enhance considerably the energy that flows into dynamic flow structures. These analyses predict energy dissipation rates amplified on the order from 100 to 200 times the energy dissipation rates that would exist in a mean turbulent flow. For the unstable bursts observed downstream of the cavity restrictors, we have mapped the maximum rates of dissipation of flutuating kinetic energy for various downstream station. The ratio of energy dissipation rates within the vortex bursts to the mean energy dissipation rates range from 28.3 at 2 mm downstream of the forward restrictor, to 25.6 at 3 mm, 15.2 at 5 mm, 12.8 at 7 mm, and 5.96 at 12 mm downstream of the forward restrictor.

VI. Maximum Entropy Results

The maximum entropy spectral analysis technique was performed on a set of 48 time measurements taken with a Hewlett-Packard Model 3582A Spectrum Analyzer with the probe at 2 and 3 mm downstream of the forward restrictors, at various vertical stations in the lower shear layer. These velocity time samples were obtained in the region of the shear layer toward the centerline of the flow, well above the critical layer. At this vertical location, the time between bursts is greater than the extent of the bursts. Burg's[12] method, as developed by Haykin and Kesler,[13] was employed to identify the frequency characteristics of the velocity burst signals obtained from the spectrum analyzer. Figure 5 presents a representative sample of the 48 time measurements taken at an axial station of 2 mm downstream from the forward restrictors. The bar on Fig. 5 indicates the time data samples from which the maximum entropy power spectral density was calculated. The time samples for each set of data to be analyzed were selected subjectively, at representing periodically ordered velocity bursts. We suspect that in the future a more objectively based criterion will be developed for the selection of the data representing an unstable burst.

The X-configuration velocity probe was placed at 0.1 mm intervals in vertical position, from -23.5 mm to -22.8 mm below the flow centerline at a downstream position of 2 mm. At each vertical position, three independent sets of time-sampled data were obtained, each representing an unstable velocity "burst." Each set of time-sampled data was then analyzed by the maximum entropy method to extract the frequencies imbedded within the data. Figure 6 presents a typical result for the analysis of a given set of time-sampled data. Table 3 presents the overall results obtained by this method of analysis and are presented for comparison with future measurements in similar regions.

It is interesting to compare the various frequencies of the most unstable disturbance obtained from Michalke's calculation and Miksad's experiments, indicated in Table 2, with the results obtained from the maximum entropy analysis of the "bursts" of turbulence obtained in the time samples. Each of the experimental frequencies in Table 3 at the axial station of 2 mm was normalized by the fundamental frequency $fn = 1110$ Hz, obtained from the experimentally measured momentum thickness and Miksad's value for the most unstable Strouhal number for the $\tanh(y)$ profile, Eq. (3). Then each set of frequency values obtained for each specific location was averaged. The results are presented in Fig. 7, where the ratio of experimental frequency to fundamental frequency is plotted as a function of vertical position. These results indicate the presence of the subharmonic disturbance, $fn/2$, quite dramatically while the frequencies, $3fn/2$, $5fn/2$ and $7fn/2$ are also indicated. It is interesting to note that the fundamental frequency representing the Tollmein-Schlichting waves is only weakly indicated.

The results presented in Fig. 7 provide experimental evidence that the processes occurring in the free shear layer at a distance of 2 mm downstream of the forward restrictor appear as a subharmonic cascade from the initial subharmonic, $fn/2$, of the fundamental frequency, through the range of higher subharmonics, $3fn/2$, etc. These are the distinctive character-

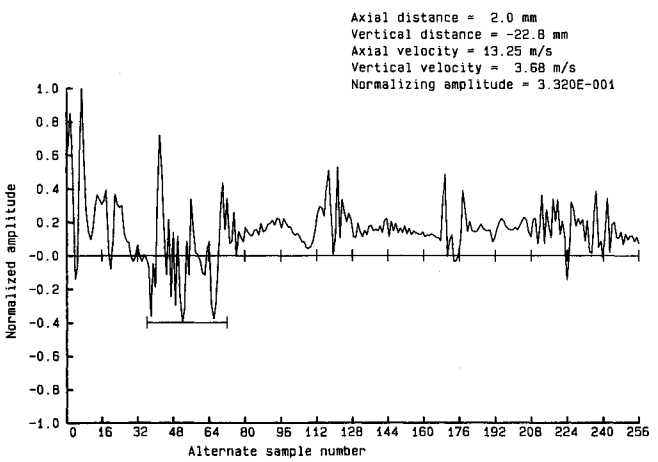

Fig. 5 Time samples of the axial velocity at 2 mm downstream and 22.8 mm below the flow centerline indicating flow structures or velocity bursts.

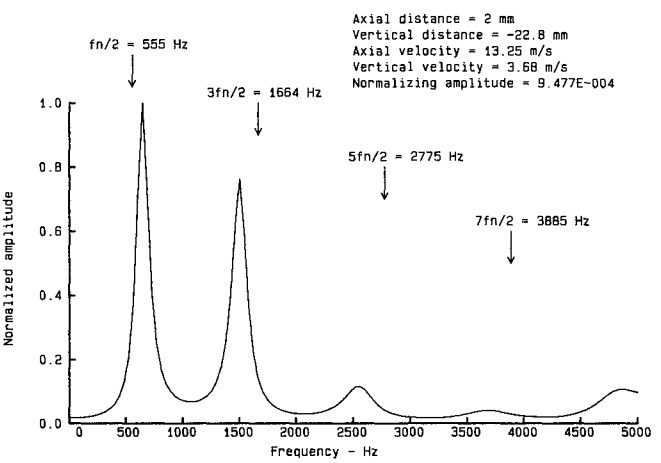

Fig. 6 Results of the application of the maximum entropy method for dominant frequencies within unstable vortices at various vertical stations at an axial station 2 mm downstream of the forward restrictors.

Table 3 Spectral components in coherent bursts in an internal free-shear layer

Axial station, mm	Vertical station mm	Burst sample	*f*1, Hz	*f*2, Hz	*f*3, Hz	*f*4, Hz	*f*5, Hz
2	−22.8	a	680	——	1520	2560	4840
		b	680	——	1720	2480	3760
		c	720	——	1760	3000	4480
	−22.9	a	——	1200	1800	2800	4400
		b	440	1160	2080	2960	3960
		c	440	——	1800	2680	3160
	−23.0	a	400	——	1520	2480	3240
		b	——	——	1320	2920	4240
		c	640	——	1640	——	——
	−23.1	a	600	1240	2000	2560	3680
		b	480	——	1400	2240	4120
		c	——	100	——	3120	——
	−23.2	a	840	1400	2080	2560	3240
		b	560	1120	1960	2560	3680
		c	560	——	2040	3000	——
	−23.3	a	680	1160	1680	2200	3240
		b	400	1280	1640	3640	4560
		c	480	1200	——	2600	3640
	−23.4	a	720	1120	2320	3520	——
		b	680	——	1360	2880	3440
		c	560	——	1320	2960	——
	−23.5	a	800	——	1920	——	3720
		b	720	1280	——	——	4280
		c	560	——	2120	——	4400
3	−22.8	a	920	1360	1920	3280	4160
		b	680	——	1800	3520	4520
		c	400	920	1720	3240	——
	−22.9	a	640	1520	2320	——	4000
		b	680	1480	2280	2920	——
		c	480	1440	——	3200	——
	−23.0	a	680	——	2320	——	——
		b	440	——	1440	——	3120
		c	400	——	1520	——	3360
	−23.1	a	——	880	2160	3040	4000
		b	640	1360	——	——	——
		c	480	1240	——	3040	4040
	−23.2	a	——	1160	——	2200	3520
		b	600	——	——	2120	3000
		c	360	1360	——	2000	3160
	−23.3	a	——	——	1400	2880	4000
		b	760	1360	——	2400	3720
		c	440	——	1600	2520	3680
	−23.4	a	920	——	1880	3240	——
		b	360	1240	1880	3360	——
		c	520	——	——	2720	3400
	−23.5	a	720	——	1680	——	2920
		c	680	1280	2000	2800	3680

istics of a nonlinear bifurcation process of period doubling, leading from the unstable state in the shear layer, into dissipative structures, and on into chaotic behavior (Bergé, Pomeau, and Vidal[14].)

In the analyses of Herbert[15,16] and the experiments of Nishioka and Asai,[17] the fundamental frequency is associated with the two-dimensional Tollmein-Schlichting wave for wall-bounded shear layers, and the subharmonic frequencies are associated with the development of longitudinal spiral vortices. It is therefore appropriate to explore evidence of the presence of spiral vortices in the internal free-shear layers employed in this study.

VII. Spiral Vortices in an Internal Free-Shear Layer

The Reynolds shear stress profile across the upper and lower shear layers at several locations downstream of the forward restrictors are shown in Fig. 3. We have interpreted the Reynolds shear stress profile in the lower shear layer at 2 mm downstream of the forward restrictors as the results produced by a set of four counter-rotating spiral vortices with axes in the axial direction. This interpretation is arrived at as follows.

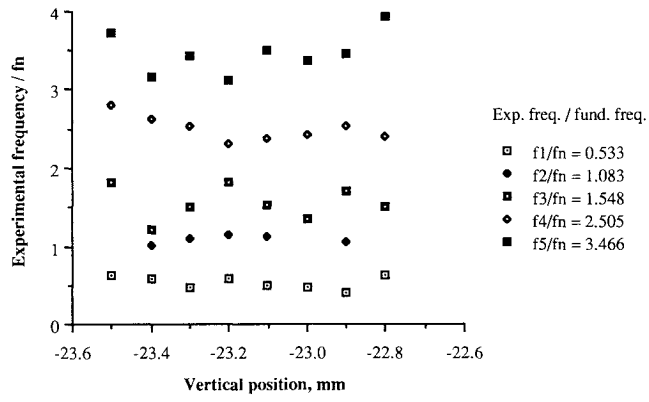

Fig. 7 Frequencies from the maximum entropy method normalized by the fundamental frequency from Miksad's results. Each data point represents an average of the frequencies from three sets of time-sampled data for each vertical position shown.

Consider the Reynolds shear stress profile in the lower shear layer at 2 mm downstream of the forward restrictors. As the X-film sensors are brought down along a vertical plane between the first pair of vortices, the Reynolds shear stress is produced by the cross correlation between the axial velocity fluctuations, u', and the vertical velocity fluctuations, v', induced by this pair of vortices in the positive vertical direction. The resulting Reynolds shear stress, $-\langle u'v' \rangle$, will then be negative. As the sensors move to the central axis between the four vortices, the contributions of the vertical velocity fluctuations by the upper and lower pairs of vortices will cancel, yielding a zero value for the Reynolds shear stress, as indicated in Fig. 3. As the sensors move further down the profile, the Reynolds stress is again produced by the cross correlation between the axial velocity fluctuation, u', and the vertical velocity fluctuation, v', this time in the negative y direction, induced by the second pair of axial vortices. This would yield a positive Reynolds stress, $-\langle u'v' \rangle$, again as indicated in Fig. 3.

With this interpretation, the profiles at 2 mm and at 7 mm then suggests the presence of paired, counter-rotating, axially directed, spiral vortices, above and below the critical layer at each of the specified locations. These vortex structures were reported by Isaacson[18] in a study of the breakup of liquid droplets under the action of the counter-rotating vortices present at the forward edge of the cavity flow. The observed vortices are angled along the direction of the steep shear layer at the forward restrictor edge and move radially out of the plane of the centerline in a short distance downstream, and therefore may only partially appear in the plane of measurement at 3 mm or more downstream of the restrictors.

Recently, Herbert[15,16] and Orszag and Patera[19] studied spiral vortices as secondary instabilities produced from primary Tollmein-Schlichting waves in wall-bounded shear layers. In comparison, the measurement of frequencies within the turbulent bursts in the free-shear layer over the lower restrictors indicates the presence of subharmonic frequencies that may represent transient sprial vortices, without a significant contribution from the fundamental frequency as calculated from the fundamental Strouhal number. It appears that spiral vortices produced along the forward shear layers in an internal cavity flow originate from a mechanism which is not dependent upon the existence of two-dimensional roll vortices representing the fundamental mode of instability of the shear layer. The large two-dimensional roll-vortex structures observed in internal cavity flows come into existence further downstream from the sharp edge of the restrictors, and the mechanism of interaction between the spiral vortices and the two-dimensional vortex structures is presently unknown. We have found evidence (Crepeau and Isaacson[5]) that the velocity profiles established along the near region shear layers of the internal cavity flow

produce what we have called "regions of instability," which, in a deterministic sense, show unstable behavior, leading to the production of rapidly changing velocities. Outside of these regions, the flow is stable, and the velocities behave smoothly.

VIII. Conclusions

Many investigators are studying the properties of coherent structures in fluid flow, especially the formation of coherent structures within shear layers. Experimental data are presented in this paper, that provide evidence of the existence of counter-rotating longitudinal vortices along the steep shear layers in the forward region of an internal cavity flow. Application of the maximum entropy method of spectral analysis to time samples taken within unstable bursts observed along the shear layer in the forward cavity region yields subharmonic and superharmonic components of the fundamental frequency of the most unstable frequency for the hyperbolic tangent profile. Comparison of these components with the results of the analysis of wall shear layers suggests the existence of longitudinal spiral vortices of a transient, dynamic nature. Finally, the agreement of measured velocity profiles with Stuart theoretical profiles suggests a method for analytically determining velocity gradients within steep internal shear layers. With the experimental verification of analytical velocity profiles, we will be able to investigate the thermodynamic and hydrodynamic properties of a free-shear layer with deterministic methods that require considerably less computing power than is normally required for the complete numerical solution of the near flowfield.

References

[1]Komerath, N. M., Ahuja, K. K., and Chambers, F. W., "Prediction and Measurement of Flows Over Cavities – A Survey," AIAA Paper 87-0166, Jan 1987.

[2]Stuart, J. T., "On Finite Amplitude Oscillations in Laminar Mixing Layers," *Journal of Fluid Mechanics,* Vol. 29, Part 3, 1967, pp. 417–440.

[3]Miksad, R. W., "Experiments on the Nonlinear Stages of Free-Shear-Layer Transition," *Journal of Fluid Mechanics,* Vol. 29, Part 3, 1967, pp. 417–440.

[4]Wooley, J. P and Karamcheti, K. "Role of Jet Stability in Edgetone Generation," *AIAA Journal,* Vol. 12, Nov. 1974, pp. 1457–1458.

[5]Crepeau, J. C. and Isaacson, L. K., "Unstable Bursts in the Near Region of an Internal Free Shear Layer," AIAA Paper 88-3578.

[6]Townsend, A. A., *The Structure of Turbulent Shear Flow,* Cambridge University Press, Cambridge, UK, 1976 pp. 46–49.

[7]Michalke, A., "On the Inviscid Instability of the Hyperbolic Tangent Velocity Profile," *Journal of Fluid Mechanics,* Vol. 19, 1964, pp. 543–556.

[8]Benney, D. J., "A Non-Linear Theory for Oscillations in a Parallel Flow," *Journal of Fluid Mechanics,* Vol. 10, 1961, pp. 209–236.

[9]Benney, D. J., "The Evolution of Disturbances in Shear Flows at High Reynolds Number," *Studies in Applied Mathematics,* Vol. 70, 1984, pp. 1–19.

[10]Benney, D. J. and Gustavsson, L.H., "A New Mechanism For Linear and Nonlinear Hydrodynamic Instability," *Studies in Applied Mathematics,* Vol. 64, 1981, pp. 185–209.

[11]Greenspan, H. P. and Benney, D. J., "On Shear-Layer Instability, Breakdown and Transition," *Journal of Fluid Mechanics,* Vol. 15, 1963, pp. 133–153.

[12]Berg, J. P., "Maximum Entropy Spectral Analysis," 37th Annual International Meeting, Society of Exploration Geophysics, Oklahoma City, OK, 1967.

[13]Haykin, S. and Kesler, S., "Prediction-Error Filtering and Maximum Entropy Spectral Estimation," *Nonlinear Methods of Spectral Analysis,* edited by S. Haykin, Springer-Verlag, Berlin, 1983, pp. 9–72.

[14]Bergé, P., Pomeau, Y., and Vidal, C., *Order with Chaos,* Wiley, New York, 1984, pp. 210–217.

[15]Herbert, T., "Secondary Instability of Plane Channel Flow to Subharmonic Three-Dimensional Disturbance," *The Physics of Fluids,* Vol. 26, April 1983, pp. 871–874.

[16]Herbert, T., "Subharmonic Three-Dimensional Disturbances in Unstable Plane Shear Flows," AIAA Paper 83-1739.

[17]Nishioka, M. and Asai, M., "Three-Dimensional Wave-Disturbances in Plane Poiseuille Flow," *Laminar-Turbulent Transition,* edited by V. V. Kozlov, Springer-Verlag, Berlin, 1985, pp 173–182.

[18]Isaacson, L. K., "Spiral Vortices and Liquid Breakup," *AIAA Journal,* Vol. 24, May 1986, pp. 885–860.

[19]Orszag, S. A. and Patera, A. T., "Subcritical Transitio to Turbulence in Planar Shear Flows," *Transition and Turbulence,* edited by R. E. Meyer, Academic, New York, 1981, pp. 127–146.